Experimental and Numerical Investigation of Flow under Sluice Gates

Ludovic Cassan, Gilles Belaud

Experimental and Numerical Investigation of Flow under Sluice Gates

Ludovic Cassan[1] and Gilles Belaud[2]

Abstract: The flow characteristics upstream and downstream of sluice gates are studied experimentally and numerically using Reynolds averaged Navier-Stokes two-dimensional simulations with a volume of fluid method. Special attention was brought to large opening and submergence, a frequent situation in distribution canals that is little seldom addressed in the literature. Experimental results obtained by ADV measurements provide mean velocity distributions and turbulence characteristics. The flow is shown to be mostly two-dimensional. Velocity fields were simulated using renormalization group k-epsilon and Reynolds stress model turbulence models, leading to an estimation of energy and momentum correction coefficients, head loss, and bed friction. The contraction coefficient is also shown to increase with gate opening at large submergence, which is consistent with the energy-momentum balance. This result can be used to derive accurate discharge equations.

Author keywords: Sluice gate; Experiments; Computational fluid dynamics; Contraction coefficient.

Introduction

Sluice gates are a very common way to control water level and discharge in open channels. They are also used to measure flow rates given measurements of water levels and gate opening and play a role in the capture of floating elements such as cut or detached vegetation. Engineering studies usually take into account standard formulas (e.g., Henry 1950; Bos 1989) derived from a standard energy equation and constant contraction coefficient C_c, or adjusted discharge coefficient C_d. The link between these coefficients is given by

$$C_d = \frac{Q}{BW\sqrt{2gh_0}} = C_c\sqrt{1-s'}\sqrt{\frac{H_0}{\alpha h_0}} \quad (1)$$

where $Q(m^3/s)$ = discharge; $W(m)$ = gate opening; $B(m)$ channel width; $g(m/s^2)$ = gravitational acceleration; $H_0(m)$ = upstream head; $h_0(m)$ = upstream water level; $a = W/H_0$ = relative opening; $s' = h_1/H_0$ = submergence ratio at the contracted section; $h_1(m)$ = water depth at the contracted section; α = energy correction coefficient attributable to the non uniformity of the velocity distribution; $C_c = h_c/W$ = contraction coefficient; and $h_c(m)$ = minimum of the contracted stream (y_c) defined as that which carries a forward flow equivalent to the flow under the gate (Rajaratnam and Subramanya 1967).

However, submerged gates may also operate at large opening ($a > 0.5$) and may even be fully opened, causing a discontinuity in the stage-discharge relationship. In this case, Belaud et al. (2009) used the energy-momentum balance (EMB) to show that C_c should change drastically, resulting in almost no contraction when the gate lip just touches the free surface if subcritical flow is considered. The EMB is a promising approach to compute the discharge (Clemmens et al. 2003), but it requires correction coefficients and adjusted C_c (Yen et al. 2001; Lozano et al. 2009; Castro-Orgaz et al. 2010). For this, a need exists to investigate the flow structure to quantify the head losses attributable to viscosity and turbulence, and to evaluate the momentum and energy coefficients. Beyond the issue of gate calibration, determining the flow structure is also useful to study the capture of floating elements and the storage of pollutants in the recirculation zones in the case of pollution upstream of gates.

Much attention was given to free flow configurations with experimental studies (Rajaratnam and Humphries 1982; Roth and Hager 1999), potential flow solutions (Montes 1997; Vanden-Broek 1997), and numerical simulations. With the development of computer technologies, biphasic models, and turbulence models, computational fluid dynamics tools have become an efficient way to analyze flow structures in complement to experimental works. Kim (2007) and Akoz et al. (2009) studied the validity of Reynolds Average Navier–Stokes (RANS) simulations for sluice gates in free flow, focusing on pressure field C_c and mesh influence. In comparison, less has been done for submerged flow. The published works (Ma et al. 2001) did not explore a large opening, which occurs frequently in water control systems, nor did they described accurately the flow properties within the jet issued from the gate.

The objective of this note is to describe the flow properties to improve discharge computation for submerged sluice gates at a large opening. To achieve this goal, an experimental validation of the theoretical results from Belaud et al. (2009) and an estimation of corrections to apply was proposed. Because a large number of velocity measurements are necessary for a thorough description of flow for the different possible configurations, the analysis also considered RANS simulations. These simulations are validated for seven cases corresponding to various downstream conditions and openings. The validation is also done by comparing C_c from simulations with experiments on free flow in the literature. A side

[1]Assistant Professor, Institut de Mecanique des Fluides, allée du Prof. Camille Soula, 31400 Toulouse, France (corresponding author). E-mail: lcassan@imft.fr

[2]Assistant Professor, UMR G-eau, Int. Center for Higher Education in Agricultural Sciences, 2 place P. Viala, 34060 Montpellier Cedex 1, France.

result is a discussion about the validity of standard RANS simulation methods in the case of such hydraulic structures.

Material and Methods

Experimental Setup

Experiments were carried out at the hydraulic laboratory of Montpellier Agricultural Univ. The flume is 30 cm wide, 50 cm high, and 8 m long, and is composed of glass walls and a steel bottom. The sluice gate was positioned at the middle of the flume. Discharge was adjusted by a valve on the inlet pipe feeding the flume and was measured on the inlet pipe by a ultrasonic flowmeter. The tail depth was fixed by an adjustable weir at the downstream end of the flume. The gate was made of Plexiglass with sharp edges of 5 mm thickness. Gate opening varies from 2 to 24 cm, with an accuracy of ± 0.2 mm thanks to the use of prefabricated elements slid under the gate. An upstream depth of approximately 0.2 m for free flow and 0.3 m for submerged flow was chosen, corresponding to the maximum gate opening at the maximum possible discharge.

A detailed analysis of the flow was performed for configurations F-2, F-4, F-6, S-5, S-9, and S-11 described in Table 1. Velocities were measured with the Vectrino acoustic doppler velocimeter from Nortek™. The sample rate was 25 Hz. The sample volume and transmit length were chosen to ensure recommended measurement conditions, namely SNR (signal to noise ratio) greater than 20 and total counts greater than 70. These conditions were obtained for a sample volume 1.9 mm high and a transmission length of 1.2 mm. Sensor was maintained vertically with a cylindrical stem of diameter 1 cm. An accuracy of ± 0.5 mm in the vertical direction and ± 2 mm in the longitudinal direction can be reached with this setup. For each point, the three velocity components were recorded during 40 s. Although the sampling duration is rather short for an accurate estimation of turbulence moments (Garcia et al. 2007), obtaining mean velocity and turbulence intensity is sufficient (Carollo et al. 2002). Turbulence properties were computed by analyzing and averaging instantaneous data. Theoretical conditions on sampling frequency proposed by Garcia et al. (2007) were checked to obtain consistent turbulence measurements. Advanced corrections were not necessary as little noise was present in the energy spectrum. Less than 0.5 % of data were aberrant (equal to maximum velocity range) and removed.

Table 1. Description of Experiments and Runs

Run	Q (m^3/s)	U_0 (m)	W (m)	H_0 (m)	a	s	R	F
F-1	0.024	0.118	0.02	0.201	0.1	/	23569	0.084
F-2	0.045	0.227	0.04	0.203	0.20	/	45435	0.16
F-3	0.066	0.331	0.06	0.206	0.30	/	66192	0.24
F-4	0.086	0.430	0.08	0.210	0.38	/	86053	0.31
F-5	0.105	0.526	0.1	0.214	0.47	/	105139	0.38
F-6	0.124	0.618	0.12	0.220	0.54	/	123535	0.44
F-7	0.002	0.098	0.012	0.107	0.112	/	19450	0.096
S-1	0.037	0.133	0.03	0.302	0.10	0.89	39803	0.08
S-2	0.065	0.237	0.06	0.297	0.20	0.51	71025	0.14
S-3	0.058	0.212	0.06	0.286	0.21	0.63	63527	0.12
S-4	0.051	0.183	0.06	0.297	0.20	0.71	55016	0.11
S-5	0.041	0.150	0.06	0.313	0.19	0.77	44920	0.09
S-6	0.029	0.106	0.06	0.295	0.20	0.92	31763	0.06
S-7	0.044	0.159	0.09	0.292	0.31	0.92	47645	0.09
S-8	0.058	0.212	0.12	0.289	0.41	0.93	63527	0.12
S-9	0.073	0.265	0.15	0.289	0.52	0.94	79408	0.15
S-10	0.088	0.318	0.18	0.289	0.62	0.94	95290	0.19
S-11	0.102	0.371	0.21	0.293	0.72	0.92	111172	0.22
S-12	0.117	0.424	0.24	0.289	0.83	0.94	127054	0.25
S-13	0.033	0.118	0.03	0.302	0.10	0.50	35513	0.07
S-14	0.029	0.106	0.03	0.303	0.10	0.59	31763	0.06
S-15	0.025	0.092	0.03	0.309	0.10	0.68	27508	0.05
S-16	0.021	0.075	0.03	0.308	0.10	0.78	22460	0.04
S-17	0.076	0.275	0.09	0.266	0.34	0.79	82524	0.16
S-18	0.062	0.225	0.09	0.282	0.32	0.85	67380	0.13
S-19	0.083	0.299	0.12	0.296	0.41	0.81	89840	0.17
S-20	0.103	0.374	0.15	0.282	0.53	0.85	112301	0.22

Note: Runs F1–7 and S1–20 correspond to free and submerged flow, respectively. Notation: q = discharge; U_0 = upstream velocity; w = gate opening; $\mathsf{R} = u_0 H_0/\nu$ Reynolds number; ν = kinematic viscosity; $\mathsf{F} = U_0/\sqrt{GH_0}$ Froude numbers at the upstream section; $s = H_2/h_0$ submergence ratio; H_2 = downstream water depth.

Modeling Equations

Twenty-seven configurations were simulated (Table 1). A specific simulation (F-7) was performed with the conditions from Akoz et al. (2009) for comparison with PIV measurements. The RANS equations were solved with FLUENT™ 6.3 in unsteady condition. Seventy seconds of simulation time gave a constant solution in which mass balance was checked, which was difficult to obtain with steady calculation. The semi-implicit method for pressure linked equations (SIMPLE) algorithm was used for pressure fields calculation. The pressure discretization used the pressure staggering option (PRESTO!) scheme, and other equations were discretized with a second-order scheme (Fluent Inc. 2006). To track the free surface, the partial volume of fluid model was used that adopts the VOF (volume of fluid) formulation (Hirt and Nichols 1981), but differs from VOF because air flow is taken into account (Bombardelli et al. 2001). Two phases (water and air) are considered in the entire domain. The nature of fluid modifies the volume fraction of each phase in each cell of the domain. The RANS and continuity equations are solved with volume fraction average value for properties (density and kinematic viscosity). The accurate free surface position is interpolated using the geometric reconstruction scheme.

Turbulence kinetic energy (k) is defined from velocity fluctuations u' and v' in the longitudinal and vertical directions:

$$k = \frac{1}{2}(\overline{u'^2} + \overline{v'^2}) \tag{2}$$

Because of its simplicity and shorter computation time, the standard k–ε model (Launder and Spalding 1974; Rodi 1984) is generally chosen in commercial applications and was used by Ma et al. (2001) for submerged jumps. In this study, the RNG k–ε model is used because the computational overhead is minor and the model is known to be appropriate for strained flow (Fluent Inc. 2006). An anisotropic model, the Reynolds Stress Model (RSM), was also used and is expected to better describe the 2D flow near the separation point (Launder 1989). All models were parameterized with the standard values available in FLUENT. The influence of the turbulence models on velocity profile was analyzed for cases F-1 to F-7, S-5, S-9, and S-11.

Mesh

The 2D structured mesh was produced with GAMBIT software. The domain dimensions are 4×0.4 m for free flow and 6×0.6 m for submerged flow. The gate was located 3 m

downstream from the inlet boundary and is taken as the origin of the horizontal abscissas x. Fourteen different meshes were created, corresponding to the different openings and free surface position. The meshes were refined near the wall boundaries (bottom and sluice gate) and the free surface. These two zones of refined mesh require a large number of cells in the entire water domain (9,600 cells for free flow) to avoid flat cells and to fix a size ratio lower than 1.5 between two successive cells. The meshing procedure is detailed by Cassan and Belaud (2008). For free flow, the meshes were refined until the influence on C_c became negligible (less than 0.5%). The maximum error on velocity is less than 2%. The choice of this refinement is a compromise between computational time and accuracy on C_c. The wall functions defined by Launder and Spalding (1974) were used. The mesh was constructed to verify the condition $12 < y^+ < 250$, with $y^+ = yu^*/\nu$, u^* = shear velocity, and y = vertical coordinate. Because this condition is not easy to obtain with a structured mesh and a flow strongly accelerated under the sluice gate, the mesh was locally adapted (see Fig. 1).

Boundary Conditions

The boundary conditions are indicated in Fig. 2. Water and air are injected separately with two velocity conditions at the inlet. Results were insensitive to air velocity, which was finally set to zero. A power law profile was given to the water inlet velocity distribution:

$$U(y) = (\gamma + 1)U_0\left(\frac{y}{h_0}\right)^{\gamma} \tag{3}$$

in which γ = shape factor and U = horizontal velocity component. Eq. (3) ensures that the mean velocity is equal to U_0 at the inlet. γ = 0.1 was used on the basis of standard values observed in open channels. The inlet is sufficiently far from the gate to guarantee that an established flow is reached before the influence of the gate, which was verified in the domain -1.5 m $< x < -1$ m for all gate openings. To refine the mesh at the free surface, an initial guess of the mean velocity was determined on the basis of Garbrecht's (1977) formula ($C_d = 0.635\sqrt{(1 - h_1/h_0)}$).

At the downstream end, a hydrostatic pressure outlet condition was imposed through to the open channel option available in FLUENT. For submerged simulations, the downstream water depth ($h_2 = 0.15, 0.18, 0.21, 0.24$ or 0.27 m) is also imposed. The bed and the gate were considered as smooth walls, whereas the top of the domain was a pressure outlet condition. The initial and boundary turbulence kinetic energy were calculated by assuming a turbulence intensity (I) of 3% ($k = 3/2(U_0 I)^2$) (Fluent Inc. 2006), which is typical for open channel flows. The results are almost insensitive to this value as it is at least one order of magnitude lower than the turbulence produced by the strained flow under the gate. Experimental and numerical distributions of k are also close to the experimental correlation of Nezu and Nakagawa (1993) for open channel flow with both turbulence models.

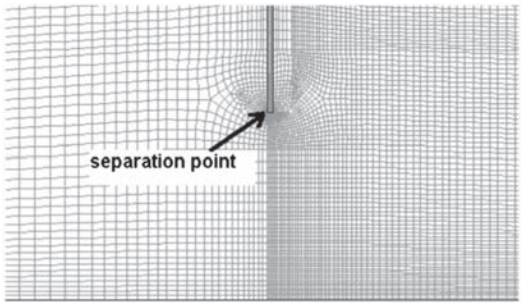

Fig. 1. Mesh under the submerged sluice gate for $a = 0.52$

Validity of 2D-RANS Simulations

Upstream of the gate, the RANS simulation is compared with the velocity measurements from Akoz et al. (2009) (Fig. 3) and with our experimental results (Figs. 4 and 5). A good agreement is generally observed except near the surface close to the gate ($-1 < X = x/W < 0$). This indicates the presence of a 3D flow compound with a low velocity recirculation zone and a highly turbulent zone as described by Rajaratnam and Humphries (1982). These regions cannot be simulated with 2D-RANS assumptions.

The low velocity recirculation has no significant influence on the velocity distribution because it has a very limited extension near the surface. The highly turbulent zone has a larger influence on the velocity profile (Fig. 5). In the corner vortices region, the average longitudinal velocity is reduced, and then it must increase at the center line. The velocity can also affect energy dissipation but, as shown further, this region has a limited contribution to the total head loss. Except in this highly turbulent zone, experimental data from Akoz et al. (2009) (Fig. 3) and Rajaratnam and Subramanya (1967) show that the 2D assumption is reasonable, which suggests a weak influence of turbulence and viscosity effects, except in the boundary layer.

Downstream of the gate, Montes (1997) and Roth and Hager (1999) showed that these 3D effects were negligible in the case of free flow. The analysis of the experimental transverse velocity distribution for configurations S-5 and S-11 at X = 2 and X = 5 leads to the same conclusion in submerged flow.

Near the separation point (Fig. 1), the flow is highly strained, and then turbulence modeling has a greater influence. The $k - \varepsilon$ and $k - \omega$ models were tested but they deviated significantly from experimental data. Indeed, these models over estimated k for velocity tending to 0 (stagnation point) (Franke et al. 2004), which is attributable to the assumption of turbulence isotropy. With a

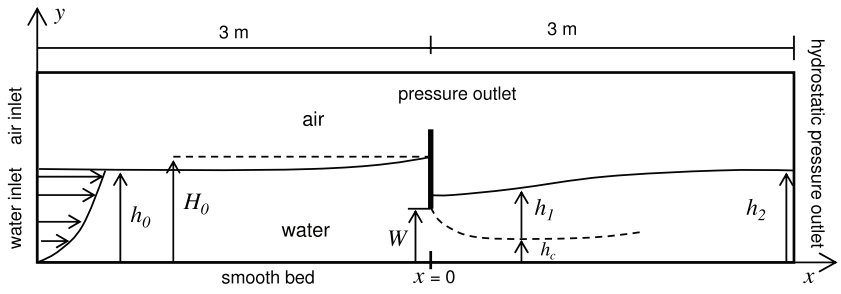

Fig. 2. Domain and boundary conditions for 2D RANS simulation of the submerged sluice gate

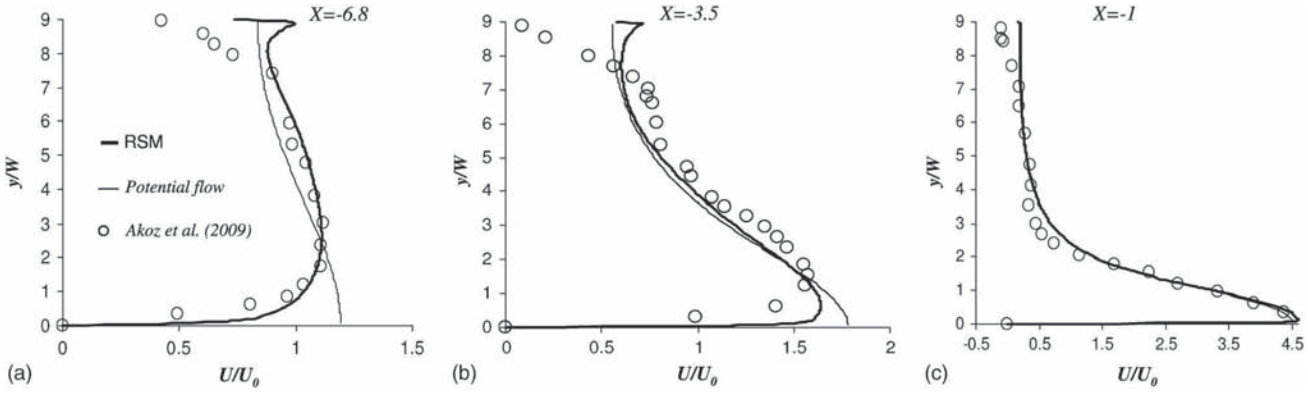

Fig. 3. (a), (b), and (c) Water longitudinal velocity profile upstream of the gate for flow condition proposed by Akoz et al. (2009). Comparison between measurement and present calculations (run F-7) and potential flow solution (Belaud and Litrico 2008)

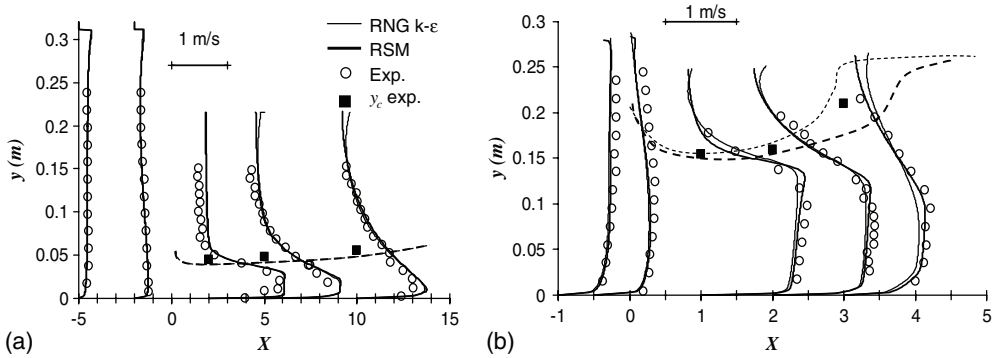

Fig. 4. Longitudinal velocity profile for submerged flow for the run S-5, $a = 0.2$, $s = 0.77$ ($X = -5, -2, 1, 5, 10$): (a) and for the run S-11, $a = 0.72$, $s = 0.93$; (b) dashed curves correspond to the contracted stream with RSM and RNG $k - \varepsilon$ models

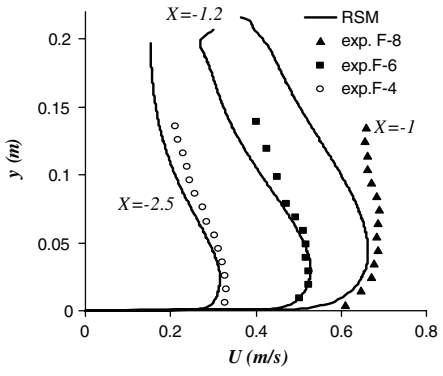

Fig. 5. Longitudinal velocity profile in free flow, for three openings, upstream of the gate at $x = -0.1$ m (with RSM model for RANS results)

$k - \varepsilon$ model, Akoz et al. (2009) found a contraction coefficient of 0.72 (for $a = 0.112$), which is above usually observed values (Montes 1997; Defina and Susin 2003). In free flow (configuration F-2), simulated C_c is approximately 17% higher with $k - \varepsilon$ than with RSM, which is close to experimental data. Therefore, only results from RNG $k - \varepsilon$ and RSM models are presented in the following.

In submerged flow, both models reproduce the longitudinal velocity profiles in the jet zone, with a slight over estimation of the maximum velocity. This difference (less than 5%) may be linked to bed roughness, which was not strictly null, and possible error on discharge estimation.

From the velocity profile, the contraction stream (y_c) is calculated. These lines are plotted along with the velocity profile (Fig. 4). They are consistent with the experimental values of y_c, estimated with an accuracy of approximately 1 cm attributable to the interpolation of the measured velocities at intervals of 1 or 2 cm. The contracted section is located at $1 < X < 2$ with both models, which is similar to free flow (Roth and Hager 1999).

Both turbulence models also capture the distribution of k (Fig. 6). Smaller values were generally observed from turbulence model assumptions and the absence of filtering of ADV measurements. These discrepancies did not affect the longitudinal velocity, and then y_c. As expected, the maximum of turbulence energy and dissipation (not presented) are in the mixing region, particularly close to the contracted stream. In most simulations, RSM agrees better with experiments and provides the flow characteristics in and above the vena contracts.

Head Loss and Scale Effects

Whereas the total head loss is close to $(1 - s)H_0$, head loss (denoted ΔH) before the dissipation in the hydraulic jump is calculated by integration of pressure, velocity, and k between an upstream section ($x = -0.4$ m) and the contracted section. The dissipation in the turbulent layer on the bed is also quantified.

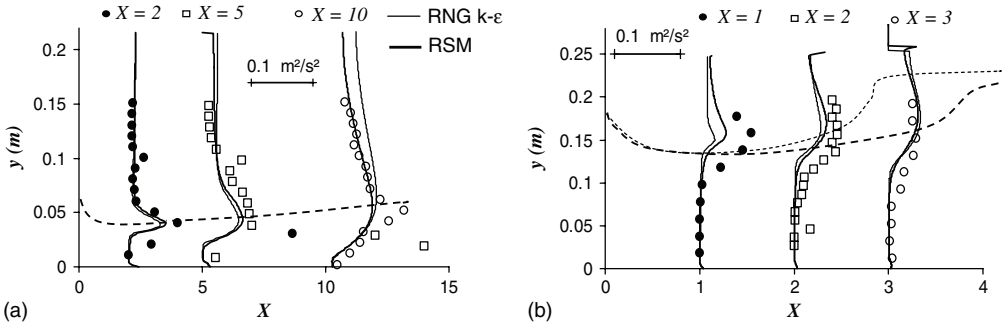

Fig. 6. Turbulence energy profile for submerged flow for run S-5, $a = 0.2$, $s = 0.77$: (a) and for run S-11 $a = 0.72$, $s = 0.93$; (b) dashed curves correspond to contracted stream (y_c) with RSM and RNG $k - \varepsilon$ models

In free flow, ΔH is primarily attributable to bed friction. The dependence of the flow on the Reynolds number is linked to the boundary layer on the bed. As suggested by Roth and Hager (1999), scale effects are significant when $W < 0.06$ m, which corresponds to $\Delta H/H_0 > 0.02$ [Fig. 7(a)]. In submerged conditions, both bed friction and mixing layer participate in energy dissipation. Values of $\Delta H/H_0$ indicate that an important part of the energy, approximately 25%, is dissipated before the contracted section [Fig. 7(b)], such as in the turbulent boundary layer and in the mixing region above the jet. For radial gates, the head loss attributable to the submerged jet is assumed to be similar to our configuration. These results were compared with the experimental correlation from Wahl (2005) to evaluate ΔH, which is reported in [Fig. 7(b)] for $a = 0.4$ m. Whereas estimations are close for large submergence, significant differences appear at small submergence. Wahl (2005) pointed out the necessity to investigate more precisely such situations, and RANS simulations provide a first response for that. For the energy momentum balance presented further, note that the scale effects may modify the velocity coefficients (α and β). However, these coefficients have a limited influence on C_c. The head losses might be used in the EMB (Belaud et al. 2009), but the influence on C_c is observed to be weak if the bed friction is added in the momentum balance. Bed shear stress can be calculated using Von Karman's equation and the approximation of the classical wall-law (Cassan and Belaud 2010). To simplify the method, head loss and bed friction have been omitted.

Correction Factors and Contraction Coefficient

The simulations provide correction coefficients attributable to the non uniformity of the velocity distribution, respectively α and β for energy and momentum corrections, and the shear exerted by the bed. At the upstream section ($x = -0.4$ m), in the established flow these coefficients are deduced by fitting a power law on the computed velocity profiles ($\gamma = 1/7$) [Eq. (3)], giving α and β equal to 1.045 and 1.016, respectively. At the contracted section, α is larger for submerged flow than for free flow, because of the mixing layer. From RNG $k - \varepsilon$ simulations, mean values of α and β are obtained, respectively 1.038 and 1.014.

For the case of free flow, the RANS simulations correctly reproduced the variation of C_c, even at small openings, because real fluid effects have a significant influence. The discrepancy between RANS and experimental results, which is less than 3 %, can be explained by the fact that the gate is not perfectly sharp-crested. Contraction coefficient is also calculated from EMB as described in Belaud et al. (2009). Applying the EMB using $s' = h_1/H_0$ is more convenient, whereas $s = h_2/H_0$ was used at the downstream boundary in the RANS simulations. The relationship between s' and s is deduced from the momentum equation written between the contracted section and the downstream section. RANS simulations give very close values of s'/s [Fig.8(b)].

Simulated C_c and calculated C_c from EMB are compared in Fig. 8(b). Taking account of α and β corrections slightly improves the determination of C_c, from which discharge coefficients can be deduced. Both approaches clearly show the increase of C_c with gate opening at large submergence, which is a key result. As shown by Belaud et al. (2009), submergence does not influence significantly the contraction coefficient for fully submerged conditions. Therefore, for practical applications, the analytical method proposed by Belaud et al. (2009) is still appropriate to compute C_c. At a small opening, C_c depends little on a, and it is slightly above the standard value of 0.61. Such values are also reported by Lozano et al. (2009), who obtained C_c between 0.629 and 0.659 by calibration on field data. At a large opening, experiment S-11 gives $C_c = 0.73$ for

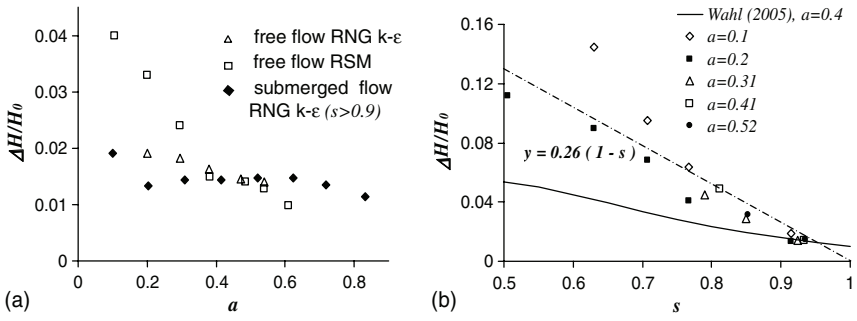

Fig. 7. Head loss (ΔH) between upstream and contracted sections as a function of relative opening: (a) and submergence; (b) Simulations were performed with RNG $k - \varepsilon$ model

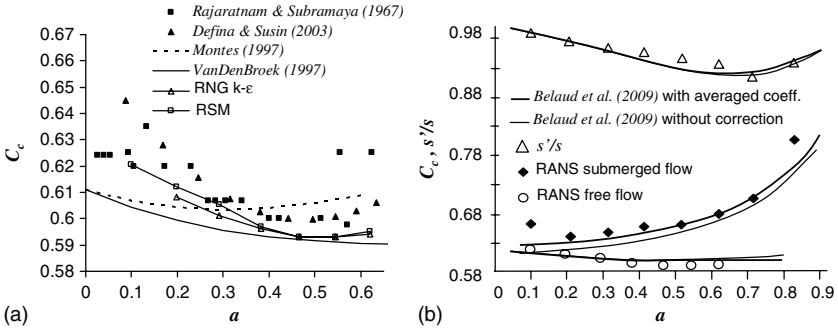

Fig. 8. (a) contraction coefficients for the case of free flow (RANS simulations); (b) case of submerged flow ($s = 0.93$): calculated contraction coefficients with RANS simulations and EMB formulation. The turbulence model is RNG $k - \varepsilon$

$a = 0.72$ and $C_d = 0.31$, which is verified by both EMB and RANS simulations (RSM or RNG $k - \varepsilon$). When a = 0.72 and $s = 0.9$, EMB gives a discharge coefficient of 0.33 compared with 0.26 (-21%) with Garbrecht's equation and 0.47 with Swamee's (1992) formula ($+42\%$).

Conclusion

The following conclusions are drawn from the present study.

- The choice of the turbulence model is important, as standard $k - \varepsilon$ and $k - \omega$ models largely over estimate the contracted stream thickness.
- With RSM and RNG $k - \varepsilon$, velocity profiles are calculated accurately. The velocity profiles are then used to estimate energy and momentum coefficients, head loss, friction forces, and contraction coefficient. Such coefficients are used to parameterize the energy-momentum balance. Scale effects may also be analyzed.
- In the case of submerged flow with large gate opening, C_c should not be considered in free flow (around 0.61) because it was verified to largely increase with gate opening. The EMB is a method to evaluate this variation and to calculate accurate discharge coefficients.

Acknowledgments

This study was carried out within project Algequeau (ANR-06-ECOT-001) supported by the French National Research Agency (ANR), which is gratefully acknowledged.

References

Akoz, M., Kirkgoz, M., and Oner, A. (2009). "Experimental and numerical modeling of a sluice gate flow." *J. Hydraul. Res.*, 47(2), 167–176.

Belaud, G., Cassan, L., and Baume, J.-P. (2009). "Calculation of contraction coefficient under sluice gates and application to discharge measurement." *J. Hydraul. Eng.*, 135(12), 1086–1091.

Belaud, G., and Litrico, X. (2008). "Closed-form solution of the potential flow in a contracted flume." *J. Fluid Mech.*, 599, 299–307.

Bombardelli, F. A., Hirt, C. W., and García, M. H. (2001). "Discussion of 'computations of curved free surface water flow on spiral concentrators'." *J. Hydraul. Eng.*, 127(7), 629–630.

Bos, M. (1989). *Discharge Measurement Structures*, 3rd Ed. International Institute for Land Reclamation and Improvement. Wageningen, The Netherlands.

Carollo, F. G., Ferro, V., and Termini, D. (2002). "Flow velocity measurements in vegetated channels." *J. Hydraul. Eng.*, 128(7), 664–673.

Cassan, L., and Belaud, G. (2010). "Experimental and numerical studies of the flow structure generated by a submerged sluice gate." *Proc. 1st Eur. IAHR Cong.*, Edinburgh, UK.

Cassan, L., and Belaud, G. (2008). "Rans simulation of the flow generated by sluice gates." *Hydraulic structure: Proc. 2nd Int. Junior Res. and Eng. Workshop on Hydraulic Structure (IJREW'08)*, S. Pagliara, ed., Edizioni Plus—Pisa University Press, Pisa, Italy, 217–225.

Castro-Orgaz, O., Lozano, D., and Mateos, L. (2010). "Energy and momentum velocity coefficients for calibrating submerged sluice gates in irrigation canals." *J. Irrig. Drain. Eng.*, 136(9), 610–616.

Clemmens, A. J., Strelkoff, T., and Repogle, J. (2003). "Calibration of submerged radial gates." *J. Hydraul. Eng.*, 129(9), 680–687.

Defina, A., and Susin, F. (2003). "Hysteretic behavior of the flow under a vertical sluice gate." *Phys. Fluid.*, 15(9), 2541–2548.

Fluent Inc. (2006). "FLUENT 6.3 User's Guide."

Franke, J., Hirsch, C., Jensen, A., Krus, H., Schatzmann, M., Westbury, P., Miles, S., Wisse, J., and Wright, N. (2004). "Recommendations on the use of CFD in wind engineering." *The Int. Conf. Urban Wind Engineering and Building Aerodynamics, von Karman Institute*, J. van Beeck (ed.), Sint-Genesius-Rode, Belgium.

Garbrecht, G. (1977). "Discussion of 'Discharge Computations at River Control Structures'." *J. Hydraul. Div.*, 103(12), 1481–1484.

Garcia, C., Cantero, M., Nino, Y., and Garcia, M. (2007). "Closure to "turbulence measurements with acoustic Doppler velocimeters"." *J. Hydraul. Eng.*, 133(11), 1289–1292.

Henry, H. R. (1950). "Discussion: 'Diffusion of submerged jet'." *Trans. Am. Soc. Civ. Eng.*, 115, 687–694.

Hirt, C., and Nichols, B. (1981). "Volume of fluid (VOF) method for the dynamics of free boundaries." *J. Comput. Phys.*, 39(1), 201–225.

Kim, D. (2007). "Numerical analysis of free flow past a sluice gate." *KSCE J. Civ. Eng.*, 11(2), 127–132.

Launder, B. (1989). "Second-moment closure: present and future?" *Int. J. Heat Fluid Flow*, 10(4), 282–300.

Launder, B., and Spalding, D. (1974). "The numerical computation of turbulent flows." *Comput. Methods Appl. Mech. Eng.*, 3(2), 269–289.

Lozano, D., Mateos, L., Merkley, G. P., and Clemmens, A. J. (2009). "Field calibration of submerged sluice gates in irrigation Canals." *J. Irrig. Drain. Eng.*, 135(6), 763–772.

Ma, F., Hou, Y., and Prinos, P. (2001). "Numerical calculation of submerged hydraulic jumps." *J. Hydraul. Res.*, 39(5), 493–501.

Montes, J. (1997). "Irrotational flow and real fluid effects under planar sluice gates." *J. Hydraul. Eng.*, 123(3), 219–231.

Nezu, I., and Nakagawa, H. (1993). *Turbulence in open-channel flows*, IAHR Monograph, Balkema, Netherlands.

Rajaratnam, N., and Humphries, J. (1982). "Free flow upstream of vertical sluice gates." *J. Hydraul. Res.*, 20(5), 427–437.

Rajaratnam, N., and Subramanya, K. (1967). "Flow equation for the sluice gate." *J. Irrig. Drain. Div.*, 93(3), 167–186.

Rodi, W. (1984). *Turbulence models and their application in hydraulics*, Int. Association for Hydraulic Research (IAHR), Delft, The Netherlands.

Roth, A., and Hager, W. (1999). "Underflow of standard sluice gate." *Exp. Fluids*, 27(4), 339–350.
Swamee, P. K. (1992). "Sluice-gate discharge equations." *J. Irrig. Drain. Div., ASCE*, 118(1), 56–60.
Vanden-Broeck, J. (1997). "Numerical calculation of the free-surface flow under sluice gate." *J. Fluid Mech.*, 330(1), 339–347.
Wahl, T. (2005). "Refined energy correction for calibration of submerged radial gates." *J. Hydraul. Eng.*, 131(6), 457–466.
Yen, J., Lin, C., and Tsai, C. (2001). "Hydraulic characteristics and discharge control of sluice gates." *J. Chin. Inst. Eng.*, 24(3), 301–310.